npj | climate and atmospheric science

www.nature.com/npjclimatsci

ARTICLE OPEN

Check for updates

Tropical cyclones over the South China Sea suppress the monsoonal rainfall in southern China

Xinyu Li[1,2]✉, Riyu Lu[3,4], Guixing Chen[5,6] and Ruidan Chen[5,6]

The tropical cyclones (TCs) often cause intense rain and destructive winds. While these catastrophic weather conditions capture our attention, the less-known impact of TCs remains overlooked. This study reveals that TCs have a notable suppressive effect on monsoonal rainfall in southern China when they traverse the South China Sea. This phenomenon can be attributed to the influence of these mesoscale disturbances on the quasi-stationary, large-scale monsoonal circulation, which alters the moisture pathway. Furthermore, the case-by-case analysis indicates that ~76% of TCs correspond to rainfall reduction, whereas the other 24% correspond to rainfall increase. The latter is due to the concurrent occurrence of another independent influencing factor: extratropical cyclonic anomalies that promote enhanced rainfall through favoring lower-tropospheric moisture convergence. This study suggests that TCs, as mesoscale disturbances, can change the moisture channel that is usually controlled by quasi-stationary and large-scale monsoonal airflows, and suppress the adjacent land rainfall over China.

npj Climate and Atmospheric Science (2023)6:207 ; https://doi.org/10.1038/s41612-023-00534-9

INTRODUCTION

The tropical cyclone (TC) is an intense weather system, with a diameter of around 100–2000 km and a lifespan of about one week. TCs often cause devastating weather, such as heavy rainfall, damaging winds, and even tornadoes[1–8]. There are generally two types of TC rainfall. The first type is directly induced by the TC core or its remnants. When TCs make landfall, they lead to this kind of rainfall, particularly over coastal areas. The second type is known as the remote, distant rainfall[9,10] or the predecessor rain events[11–13]. That is, TCs induce heavy rainfall at large distances from the TC vortex, even if they do not make landfall. A typical remote rainfall event is a result of the interaction between the outer airflows of a TC and extratropical disturbances[9,10] or local topography[14,15]. Both types of TC-associated rainfall are observed globally, including regions such as East Asia[10,16–18], South Asia[18–20], and North America[11,18,21]. They have been extensively investigated from case studies and synoptic climatology perspectives[11–13,22–25]. Furthermore, a TC is also accompanied by subsidence airflows on their periphery[26–28]. This implies that TCs may also have the potential to suppress rainfall, while this aspect of TCs has only been noticed by certain studies in certain areas[29]. Our understanding of this particular impact of TCs, especially from the perspective of synoptic climatology, appears to be deficient.

On the other hand, the monsoonal circulation is on a planetary scale and quasi-stationary[30,31]. It results in prolonged periods of rainfall, i.e., rainy seasons, and plays a crucial role in shaping regional climates. In comparison to the expansive monsoonal airflows, TCs are significantly smaller in size and have a shorter lifespan. Despite this, this study demonstrates that these strong disturbances have the ability to alter the large-scale monsoonal circulation and exert a substantial influence on the extensive monsoonal rainfall.

Many monsoonal regions are frequently affected by TCs. One such region is Southern China (SC), one of the most densely populated and economically developed regions in China. During May–August, the southwesterly monsoonal airflows, as a part of the Asian summer monsoon, carry abundant water vapor from the Indian Ocean and the Bay of Bengal into the SC region, resulting in heavy precipitation there[30–33]. The plentiful monsoonal rainfall makes the SC region an important commodity grain base in China. On the other hand, the TCs can attack SC and induce heavy rainfall, particularly in the coastal areas of SC. For instance, the TC-induced precipitation in the inland areas of SC contributes 5–10% to the total annual precipitation, and over 20% in the coastal regions[16,34]. These landfalling TCs include those generating in the South China Sea (SCS) and those generating in the western North Pacific and then entering into the SCS.

When focused on the huge rainfall caused by TCs, one tends to ignore another of their effects. In this study, we demonstrate that the TCs, when they are wandering around the SCS, can significantly suppress land monsoonal rainfall over the SC region by altering the monsoonal flows. One such example is TC Wayne (1986), one of the longest-lived TCs in the western Pacific and SCS. While the torrential rainfall and strong wind it brought in Taiwan drew widespread attention, the SC region experienced consistently reduced rainfall for over 2 weeks (Supplementary Fig. 1), spanning nearly the entire lifespan of Wayne. The suppression in monsoonal rainfall poses a serious threat to food production in the SC region. Despite extensive efforts to investigate reduced monsoonal rainfall or drought in SC[35–37], previous studies have provided little to no coverage of the impact of TCs on rainfall suppression in this area. The results are in sharp contrast to the previous studies that highlight the positive contribution of TC rainfall to the rainy season[38–41].

[1]Key Laboratory of Marine Hazards Forecasting, Ministry of Natural Resources, Hohai University, Nanjing, China. [2]College of Oceanography, Hohai University, Nanjing, China. [3]State Key Laboratory of Numerical Modeling for Atmospheric Sciences and Geophysical Fluid Dynamics, Institute of Atmospheric Physics, Chinese Academy of Sciences, Beijing, China. [4]College of Earth and Planetary Sciences, University of the Chinese Academy of Sciences, Beijing, China. [5]Southern Marine Science and Engineering Guangdong Laboratory (Zhuhai) and School of Atmospheric Sciences, Sun Yat-sen University, Zhuhai, China. [6]Key Laboratory of Tropical Atmosphere–Ocean System (Sun Yat-sen University), Ministry of Education, Zhuhai, China. ✉email: lixinyu@hhu.edu.cn

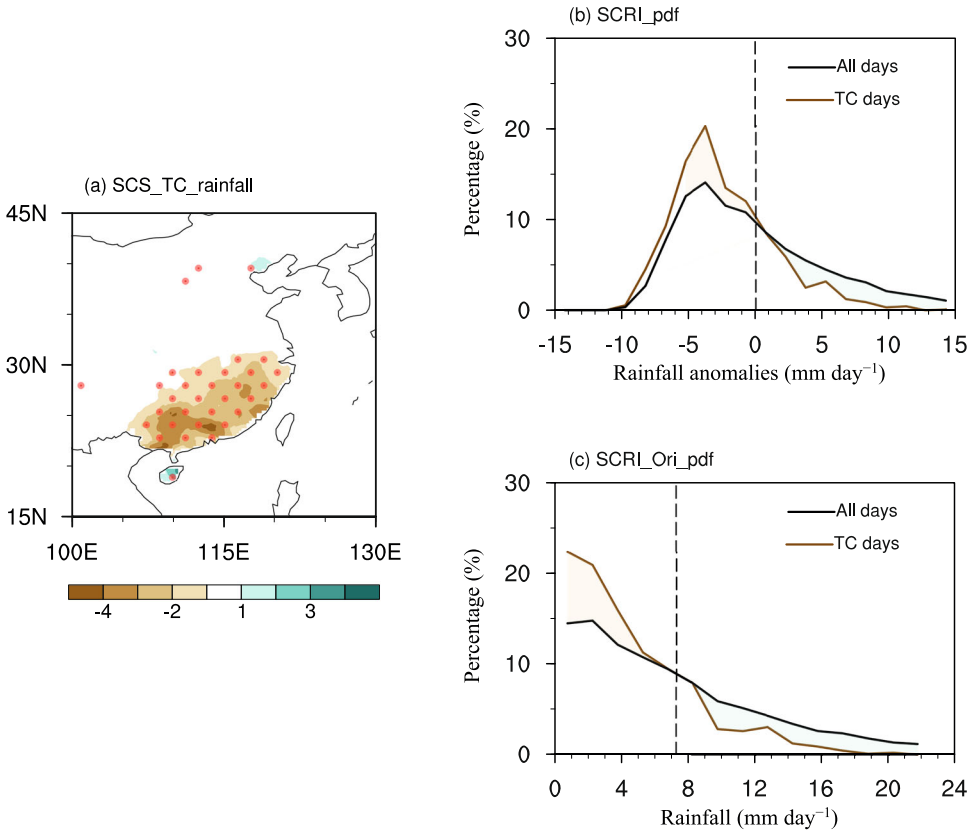

Fig. 1 Southern China rainfall associated with the SCS TCs. a Composite rainfall anomalies (shading; mm day^{-1}) over eastern China associated with TC days in the SCS during the rainy season (MJJA) of 1961–2020. Rainfall anomalies significant at the 95% confidence level are stippled as red. Probability density distributions of **b** the anomalous and **c** original SC rainfall index (SCRI) for TC days (orange line) and all MJJA days (black line). Vertical dashed lines in **b** and **c** indicate the mean of the anomalous and original SCRI on all MJJA days, respectively. Orange and cyan shadings represent the increased proportion of suppressed rainfall and the decreased proportion of enhanced rainfall, respectively.

RESULTS

Suppressed monsoonal rainfall over southern China associated with TC activities in the SCS

The SCS exhibits a substantial frequency of TCs during May–August (Supplementary Fig. 2), the rainy season of SC. It is one of the most frequent TC centers over the tropical western North Pacific, with the other center located to the east of the Philippines. These TCs are in close proximity to mainland China, but they basically have not made landfall yet. Surprisingly, these TC days correspond to strong and significantly reduced rainfall in the SC region (Fig. 1a). Compared to the composite of landfalling TCs[42,43], which lead to extremely strong positive rainfall anomalies along the coastal area, the negative rainfall anomalies associated with TCs in the adjacent SCS show an evenly distributed feature over the whole widespread SC area. The rainfall anomalies averaged over the SC region is −2.23 mm day^{-1}, accounting for 31% of the climatological mean (7.26 mm day^{-1}). In addition, there is also suppressed rainfall associated with TC activities in the east of the Philippines (Supplementary Fig. 3), but the anomalies are much weaker than those associated with TCs in the SCS. This may be because the SCS is much nearer to the SC region and the SCS TCs exert a more direct influence on the monsoonal airflows and rainfall there[44].

A comparison of the probability density distributions of the anomalous SC rainfall index (SCRI) between the SCS TC days and all MJJA days shows a clear increase in the proportion of suppressed rainfall and a decrease in the proportion of enhanced rainfall associated with these TCs (Fig. 1b). The proportion of negative SCRI increases from 60% on all days to 76% on TC days, and that of positive SCRI decreases from 40% to 24%. We also calculated the frequency of positive and negative SCRI for each TC when it appears over the SCS. There are 313 TCs counted and the mean frequencies of positive and negative SCRI for these TCs are 76.5% and 23.5%, respectively, consistent with the daily composite results. The TCs not only suppress moderate rainfall but also greatly reduce the occurrence of extreme rainfall (Fig. 1c). For instance, the proportion of the area-averaged SC rainfall >16 mm day^{-1} decreases from 10% on all MJJA days to 1.8% on TC days. These results indicate that the TC activities in the SCS effectively suppress the monsoonal rainfall over the SC region.

Mechanisms responsible for the suppressed monsoonal rainfall associated with the SCS TCs

To clarify the mechanisms behind the reduced SC rainfall caused by TCs, we analyzed the lower-tropospheric circulation and water vapor transport (Fig. 2). Climatologically, the SC region is dominated by southwesterly monsoonal airflows (Fig. 2a), which effectively transport abundant water vapor from the tropical oceans towards SC. This moisture channel contributes to the strong monsoonal rainfall over the SC region (Fig. 2d). However, the presence of TCs alters the moisture pathway in the SC region (Fig. 2b and e). These TCs greatly reduce the southwesterly monsoonal flows in southeast China and the SC region is dominated by the ridge of the subtropical high (Fig. 2b). As a result, the climatological monsoonal moisture pathway is blocked. Instead, the westerly flows from the Bay of Bengal extend eastward to the maritime continent and then shift northward towards Taiwan island and bend westward (Fig. 2e).

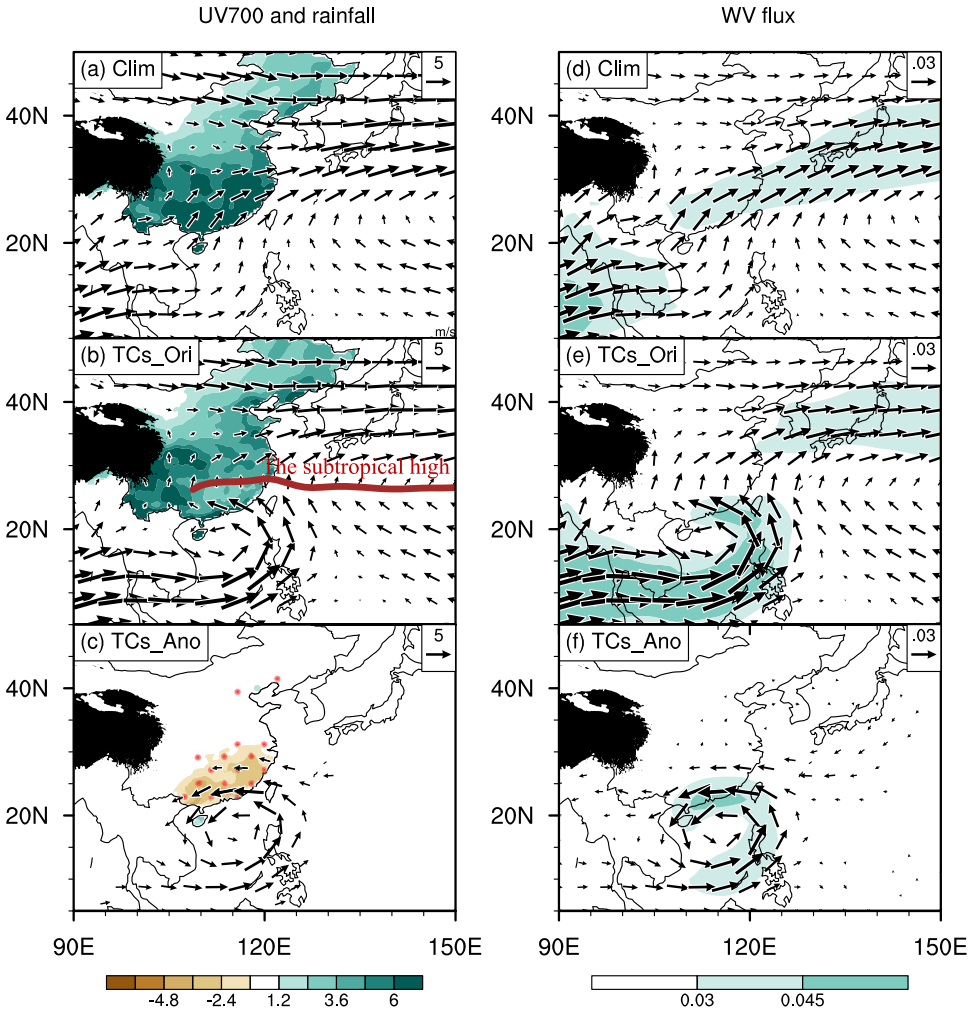

Fig. 2 UV700, rainfall and water vapor flux for climatology, TC days, and the difference between TC days and climatology. Climatology of MJJA-mean **a** 700-hPa horizontal wind (vectors; m s^{-1}) and rainfall (shading; mm day^{-1}), **d** 700-hPa water vapor flux (vectors; m s^{-1}) and its magnitude (shading; m s^{-1}) during 1961–2020. **b** and **e** are as **a** and **d**, respectively, but for the composite ones for SCS TC days. The line in **b** indicates the ridge of the western Pacific subtropical high, i.e., the line connecting points where the zonal wind equals to zero at each longitude of the high. **c** Is the difference between **b** and **a** and **f** the difference between **e** and **d**. In **c** and **f**, only vectors significant at the 95% confidence level are shown and shading significant at the 95% confidence level in **c** is stippled as red. Black shading represents mountains higher than 3000 m.

The difference between the airflows associated with TCs and the climatological mean also demonstrates the role of the SCS TCs in reducing the SC rainfall (Fig. 2c and f). The northeasterly/easterly anomalies over the SC region reduce the climatological southwesterly moisture flux. The TC-associated southeasterly onshore anomalies drop off moisture at the coastal area, but the northeasterly offshore anomalies transport moisture back to the SCS (Fig. 2f), leading to anomalous moisture divergence and suppressed rainfall over the SC region.

On the other hand, in the context of the East Asian summer monsoon region, the climatological southwesterly wind also corresponds well to ascending motion (Supplementary Fig. 4a), promoting the monsoonal rainfall. These correspondences are typical features during the rainy season over East Asia[32,33]. The TCs disrupt these well-established correspondences: the weakened southwesterly wind inhibits ascending motion over the SC region (Supplementary Fig. 4b) and reduces the SC rainfall. We explored whether storms that were northward moving resulted in a different composite to our results here. We rule out that this track feature influences our results (Supplementary Fig. 5).

The present results demonstrate that the TCs, as mesoscale strong disturbances, have the ability to modify the large-scale monsoonal circulation, thereby influencing the widespread land monsoonal rainfall. The suppressed rainfall associated with TCs in the adjacent ocean is in sharp contrast to TCs that make landfall, which bring heavy rainfall over the coastal areas[43]. Similar to the impact of certain small-scale factors, such as mountains, even slight modifications in the background airflow can result in completely different weather and climate effects, showcasing their significant influence despite their relatively small sizes.

Diversity of the SC rainfall anomalies associated with the SCS TCs

Despite the TCs in the SCS typically resulting in suppressed rainfall over the SC region, there are still over 20% of TC days that correspond to enhanced SC rainfall (Fig. 1b), though significantly fewer TC days (208 vs. 677 cases). To understand the underlying mechanism, we compare the rainfall and circulation anomalies for TC days that correspond to positive and negative SCRI (Fig. 3). The rainfall anomalies for negative SCRI resemble those for all TC days (Figs. 3b and 2c), but with more intensified values. For instance, the averaged SCRI is −3.97 mm day^{-1} for TC days with negative SCRI, which is stronger than that for all TC days (−2.23 mm day^{-1}).

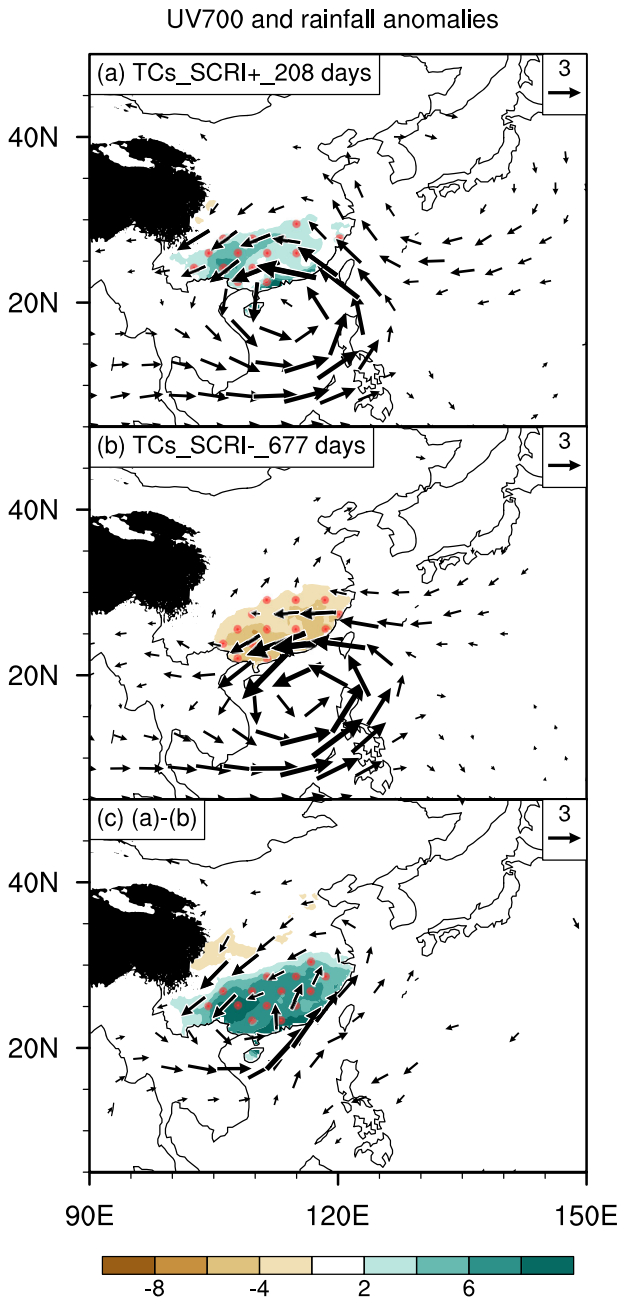

Fig. 3 UV700 and rainfall anomalies for TC days with positive and negative SCRI, as well as their difference. Composite 700-hPa horizontal wind (vectors; m s^{-1}) and rainfall anomalies (mm day^{-1}) for TC days with **a** positive and **b** negative SCRI. **c** is the difference between (**a** and **b**). Only vectors significant at the 95% confidence level are shown and shading significant at the 95% confidence level is stippled as red. Black shading represents mountains higher than 3000 m.

The lower-tropospheric circulation anomalies are also characterized by a strong and significant cyclonic anomaly over the SCS, with easterly and northeasterly anomalies to its northern flank (Fig. 3b). These TCs also suppress the monsoonal rainfall over the SC region by altering the moisture pathway (Supplementary Fig. 6b and d).

By contrast, the lower-tropospheric circulation anomalies for TC days with positive SCRI show distinctly different features (Fig. 3a). A strong and significant cyclonic anomaly also occupies the SCS, but the northern flank is located more northward. The northern flank is characterized by southeasterly and northeasterly anomalies, resembling the pattern of TC inverted trough on land[32,45]. The southeasterly anomalies are established at the east coasts in Fig. 3a, in a robust contrast to the easterly anomalies in Fig. 3b. They act to strengthen onshore moisture transport and moisture convergence over the SC region (Supplementary Fig. 6a and c), promoting enhanced rainfall there. One may concern that the enhanced rainfall may be just a result of TC centers located northward, as these positive rainfall anomalies appear to be together with the strong convection associated with the TC cores (Supplementary Fig. 7a). However, there is no clear difference in the meridional location of TCs between these two categories. The mean latitude of the TC center is 18.34°N for positive SCRI days and 18.11°N for negative SCRI days, and the median latitude of the TC center is 18.98°N and 18.40°N, respectively. These differences fail to reach statistically significant at the 95% confidence level. These results suggest that the enhanced rainfall cannot be considered as a part of strong convection in the TC core region.

We therefore investigate the other factors that should be responsible for the TC trough-like anomalies and the enhanced rainfall. The difference between these two categories gives a vital clue (Fig. 3c). It shows a widespread cyclonic anomaly over the SC region, which is largely separated from the TC-related cyclonic anomaly over the SCS. On one hand, this mid-latitude cyclonic anomaly promotes anomalous convergence in the lower troposphere and plays an important role in enhancing rainfall over the SC region. On the other hand, the cyclonic anomaly contributes to the northward extension of the northern flank of the SCS cyclonic anomaly (Fig. 3a), allowing more water vapor transport to the SC region (Supplementary Fig. 6c).

In addition, associated with the mid-latitude cyclonic anomaly, there is suppressed convection over the northern SCS (Supplementary Fig. 7c), which implies that the TCs for positive SCRI might be weaker. However, there is no clear difference in TC intensity between these two categories. The mean intensity of TCs is 42.71 kt for TC days with positive SCRI and 45.18 kt for TC days with negative SCRI, and the medians are 37.50 and 40.00 kt, respectively. These differences are not statistically significant at the 95% confidence level. Moreover, even in the absence of TCs, enhanced rainfall over the SC region also corresponds to similar circulation and convection/rainfall anomalies (Supplementary Fig. 8). These results indicate that the discrepancy between these two categories cannot be solely attributed to TC activities.

Taking into account the distance between the cyclonic anomaly and TCs, it can be inferred that the cyclonic anomaly is mainly affected by extratropical factors rather than TCs. Further results indicate that the cyclonic anomaly over North China in the upper troposphere plays an important role (Fig. 4a). A strict and detailed verification may be achieved by distinguishing environmental and TC-related fields through the potential vorticity inversion technique, as in Arakane and Hsu (2020, 2021)[46,47]. It favors the mid-latitude cyclonic anomaly in the lower troposphere (Fig. 3c), which merges with the cyclonic anomaly associated with the SCS TCs and enhances moisture transport to the SC region (Supplementary Fig. 6c). Compared to its counterpart in the lower troposphere (Fig. 3c), the upper-tropospheric cyclonic anomaly is located further north (Fig. 4b). Such northward tilted circulation anomalies are a common feature over East Asia during summer[48] and this vertical coupling between the lower and upper tropospheric anomalies may be associated with more effective energy gain from the vertically sheared jets[49–51]. In addition, the upper-tropospheric cyclonic anomaly and the vertical northward tilted feature also exist with the absence of TCs (Supplementary Fig. 9).

The present results indicate that both TCs and the extratropical anticyclonic/cyclonic anomaly exert a significant influence on the SC rainfall. The former can be further confirmed by the probability density distribution of SCRI between TC days and TC-absence days (Supplementary Fig. 10a), i.e., there is a clear increase in

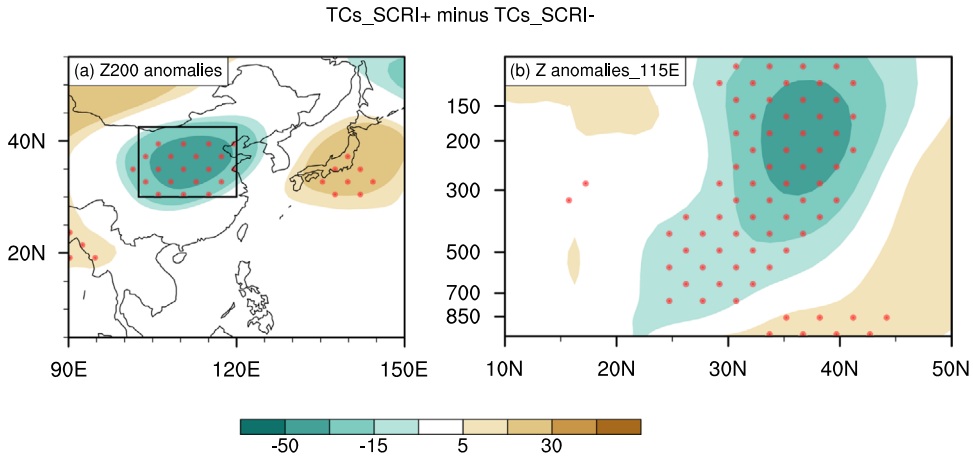

Fig. 4 Composite U200 anomalies between TC days with positive and negative SCRI. a Composite difference of 200-hPa geopotential height anomalies (shading; gpm) between TC days with positive SCRI and negative SCRI. The marked region is used to define NCCI (see the "Methods" section). **b** is as **a** but for the vertical cross-section of geopotential height anomalies along 115°E. Shading significant at the 95% confidence level is stippled as red.

suppressed SCRI and a clear decrease in enhanced SCRI for TC days. The latter can be confirmed by the correlation coefficient between SCRI and the North China cyclonic index (NCCI), which is 0.25 and statistically significant at the 95% confidence level. On the other hand, these two factors, i.e., TCs and the extratropical anticyclonic/cyclonic anomaly, tend to be independent of each other. First, the composite NCCI for TC days is $-0.10 \times 10^{-5}\,s^{-1}$, much smaller than 1.0 standard deviation ($1.89 \times 10^{-5}\,s^{-1}$). Second, the probability density distributions of NCCI show no clear difference between TC days and TC-absence days (Supplementary Fig. 10b).

As the cyclonic anomaly in the upper troposphere favors enhanced SC rainfall, an anticyclonic anomaly would play an opposite role. It would favor an anticyclonic anomaly over the SC region in the lower troposphere, which facilitates moisture divergence and suppresses the SC rainfall. To compare the impact of the anticyclonic anomaly and TCs on SC rainfall, we selected TC-absence days with NCCI smaller than −1.15 standard deviations (NCCI−) and conducted composite analyses. This criterion allows the number of anticyclonic anomaly cases (859 days), which correspond to suppressed SC rainfall, comparable to that of TCs (885 days). The rainfall anomalies associated with these NCCI− days averaged over the SC region are $-2.06\,mm\,day^{-1}$, comparable to that for TC days ($-2.23\,mm\,day^{-1}$). These results suggest that even the strong extratropical anticyclonic anomaly may play a comparable role to TCs in suppressing the SC rainfall.

Considering that the extratropical circulation anomalies also significantly affect the SC rainfall, it is necessary to further investigate the origin of the anticyclonic/cyclonic anomaly over North China. It is found that this anticyclonic/cyclonic anomaly tends to be associated with a wave train in the upper stream (Supplementary Fig. 11), which propagates eastward from the high-latitude Europe and then enters the mid-latitude Asian westerly jet. The nature of this wave train is beyond the scope of this study and remained for future exploration. In addition, it could be inferred that the concurrent occurrence of the extratropical anticyclonic anomaly over North China and TCs may lead to extremely weak SC rainfall. For instance, days with SC rainfall less than $1.0\,mm\,day^{-1}$ account for 9.36% of all MJJA days, and this percentage increases to 13.69% on TC days and further increases to 16.19% on TC days with simultaneous occurrence of the extratropical anticyclonic anomaly.

DISCUSSION

It is widely recognized that TCs often bring severe rainfall. Our findings presented here highlight another type of impact associated with TCs in the adjacent ocean, i.e., suppressing the monsoonal rainfall. The suppressed rainfall over the SC region is a consequence of the alterations of large-scale monsoonal flow induced by TCs. It is interesting that TCs, as a mesoscale weather system, have the ability to modify the large-scale monsoonal circulation and the widespread monsoonal rainfall. Our findings emphasize the high sensitivity of land monsoonal rainfall to the adjacent oceanic TCs and pose a novel perspective on the climate effect of TCs.

Given that TCs in the SCS significantly inhibit monsoonal rainfall over SC, it is expected that early (late) summer TCs may lead to a late start (early cessation) of the seasonal process of monsoonal rainfall in China. Understanding the connection between TCs and the monsoon process would be beneficial for the monsoon forecasting. Furthermore, considering the crucial role of TCs in causing rainfall anomalies over the vast monsoon area, it is imperative to monitor future changes in TC activities. Particularly, with the background of global warming, the intensity and frequency of TCs may undergo alterations[18,52–58], potentially amplifying their influence on monsoonal rainfall. In addition, TCs are also known to occur in other monsoon regions, such as the Bay of Bengal and North America, and it would be interesting to investigate their influence on the monsoonal rainfall in these areas.

METHODS

Datasets and definitions

This study utilizes daily gridded observational rainfall data from the National Climate Center of China (CN05.1)[59], with a $0.25° \times 0.25°$ horizontal resolution. Additionally, daily data from the Japanese 55-Year Reanalysis (JRA-55)[60] are employed, with a horizontal resolution of $1.25° \times 1.25°$. The TC data, with a 6-h temporal resolution (0000, 0600, 1200, and 1800 UTC), are obtained from the Joint Typhoon Warning Center and include all TCs ranging from tropical depressions to typhoons. The intensity of TC is defined as the maximum sustained wind speed in knots.

The South China Sea refers to the area 10°–22.5°N, 110°–122.5°E (Supplementary Fig. 2), and southern China (SC) encompasses the mainland area east of 105°E and between 21° and 28°N, which is similar to the location used in earlier studies[61,62]. The anomalous

southern China rainfall index (SCRI) is calculated as the rainfall anomalies averaged over the defined SC region. The North China cyclonic index (NCCI) is defined as the 200-hPa vorticity averaged over 30°–42.5°N, 102.5°–120°E (Fig. 4a). Therefore, a positive (negative) NCCI indicates a cyclonic (anticyclonic) anomaly over North China in the upper troposphere.

The analysis covers a time period from 1961 to 2020 and focuses on the May–August (MJJA) months, which coincide with the rainy season in the SC region. There are 885 days experiencing TC activities in the SCS during the analyzed period. The results associated with TC activities refer to the average of these TC days. Furthermore, daily anomalies are obtained by subtracting the climatology of a specific day from the raw data.

This study focuses on the impact of TCs on rainfall anomalies over the whole SC region, which acts as an important component of the large-scale rainy belt of East Asia during the rainy season. As moisture supply in the lower troposphere is vital for large-scale rainfall, we mainly show the moisture transport at 700 hPa, and using integration from surface to 300 hPa could obtain similar results (Supplementary Fig. 4d–f). The water vapor flux can be expressed as $\mathbf{Q} = q\mathbf{V}$, and the vertically integrated water vapor flux can be expressed as $\mathbf{Q}=\frac{1}{g}\int_{p_s}^{300}(q\mathbf{V})dp$, where g, p_s, q, and $\mathbf{V}$ are the acceleration of gravity, surface pressure, specific humidity, and horizontal wind vector, respectively. The moisture channel is represented by the magnitude of the water vapor flux.

Statistical analyses and significance

This study primarily employs composite analysis and uses the two-tailed Student's *t*-test to determine the significance of each variable at every grid point[63]. The effective sample size, denoted as N^*, at each grid point is calculated by $N^* = N \times (1-r_1)/(1+r_1)$, where N refers to the original length of the time series and r_1 represents the lag-1 autocorrelation coefficient[64]. A composite vector is considered significant if at least one of its zonal or meridional components passes the test.

DATA AVAILABILITY

All data used in this study are publicly available and can be downloaded from the corresponding websites: (1) the CN05.1 daily gridded observational precipitation data are from http://www.nmic.cn, (2) the JRA-55 reanalysis data are from https://search.diasjp.net/en/dataset/JRA55, and (3) the TC data are from http://www.usno.navy.mil/NOOC/nmfc-ph/RSS/jtwc/best_tracks/wpindex.php.

Received: 31 August 2023; Accepted: 24 November 2023;
Published online: 12 December 2023

REFERENCES

1. Lee, W.-C., Bell, M. M. & Goodman, K. E. Supercells and mesocyclones in outer rainbands of Hurricane Katrina (2005). *Geophys. Res. Lett.* **35**, L16803 (2008).
2. Yu, C.-K., Cheng, L.-W., Wu, C.-C. & Tsai, C.-L. Outer tropical cyclone rainbands associated with typhoon Matmo (2014). *Mon. Weather Rev.* **148**, 2935–2952 (2020).
3. Li, R. C. Y., Zhou, W., Shun, C. M. & Lee, T. C. Change in destructiveness of landfalling tropical cyclones over China in recent decades. *J. Clim.* **30**, 3367–3379 (2017).
4. Ruan, T., Chen, G. & Bai, L. Outer rainband formation on land ahead of typhoon Hato (2017). *J. Geophys. Res. Atmos.* **128**, e2022JD038051 (2023).
5. Tu, S. et al. Recent global decrease in the inner-core rain rate of tropical cyclones. *Nat. Commun.* **12**, 1948 (2021).
6. Utsumi, N. & Kim, H. Observed influence of anthropogenic climate change on tropical cyclone heavy rainfall. *Nat. Clim. Change* **12**, 436–440 (2022).
7. Weinkle, J. et al. Normalized hurricane damage in the continental United States 1900–2017. *Nat. Sustain.* **1**, 808–813 (2018).
8. Liu, H., Gu, J. & Wang, Y. Consistent pattern of rainfall asymmetry in binary tropical cyclones. *Geophys. Res. Lett.* **50**, e2022GL101866 (2023).
9. Bosart, L. F. & Carr, F. H. A case study of excessive rainfall centered around Wellsville, New York, 20–21 June 1972. *Mon. Weather Rev.* **106**, 348–362 (1978).
10. Wang, Y., Wang, Y. & Fudeyasu, H. The role of typhoon Songda (2004) in producing distantly located heavy rainfall in Japan. *Mon. Weather Rev.* **137**, 3699–3716 (2009).
11. Cote, M. R. Predecessor rain events in advance of tropical cyclones. Dissertation (State University of New York), (2007).
12. Galarneau, T. J., Bosart, L. F. & Schumacher, R. S. Predecessor rain events ahead of tropical cyclones. *Mon. Weather Rev.* **138**, 3272–3297 (2010).
13. Moore, B. J., Bosart, L. F., Keyser, D. & Jurewicz, M. L. Synopticscale environments of predecessor rain events occurring east of the rocky mountains in association with Atlantic basin tropical cyclones. *Mon. Weather Rev.* **141**, 1022–1047 (2013).
14. Lin, Y. & Wu, C. Remote rainfall of typhoon Khanun (2017): monsoon mode and topographic mode. *Mon. Weather Rev.* **149**, 733–752 (2021).
15. Wei, P. et al. On the key dynamical processes supporting the 21.7 Zhengzhou record-breaking hourly rainfall in China. *Adv. Atmos. Sci.* **40**, 337–349 (2023).
16. Ren, F. et al. Changes in tropical cyclone precipitation over China. J. *J. Geophys. Res.* **33**, L20702 (2006).
17. Arakane, S. et al. Remote effect of a tropical cyclone in the Bay of Bengal on a heavy-rainfall event in subtropical East Asia. *npj Clim. Atmos. Sci.* **2**, 25 (2019).
18. Guzman, O. & Jiang, H. Global increase in tropical cyclone rain rate. *Nat. Commun.* **12**, 5344 (2021).
19. Yuan, J., Zhao, D., Yang, R. & Yang, H. Predecessor rain events over China's low-latitude highlands associated with Bay of Bengal tropical cyclones. *Clim. Dyn.* **50**, 825–843 (2018).
20. Rajeev, A. & Mishra, V. On the causes of tropical cyclone driven floods in India, *Weather and Climate Extremes* (2022)
21. Gori, A., Lin, N., Xi, D. & Emanuel, K. Tropical cyclone climatology change greatly exacerbates US extreme rainfall–surge hazard. *Nat. Clim. Change* **12**, 171–178 (2022).
22. Schumacher, R. S., Galarneau, T. J. & Bosart, L. F. Distant effects of a recurving tropical cyclone on rainfall in a midlatitude convective system: a high-impact predecessor rain event. *Mon. Weather Rev.* **139**, 650–667 (2011).
23. Bosart, L. F. et al. An analysis of multiple predecessor rain events ahead of tropical cyclones Ike and Lowell: 10–15 September 2008. *Mon. Weather Rev.* **140**, 1081–1107 (2012).
24. Schumacher, R. S. & Galarneau, T. J. Moisture transport into midlatitudes ahead of recurving tropical cyclones and its relevance in two predecessor rain events. *Mon. Weather Rev.* **140**, 1810–1827 (2012).
25. Khouakhi, A., Villarini, G. & Vecchi, G. A. Contribution of tropical cyclones to rainfall at the global scale. *J. Clim.* **30**, 359–372 (2017).
26. Zhao, D., Lin, Y., Li, Y. & Gao, X. An extreme heat event induced by typhoon Lekima (2019) and its contributing factors. *J. Geophys. Res. Atmos.* **126**, e2021JD034760 (2021).
27. Guido, Z., Allen, T., Mason, S. & Méndez-Lázaro, P. Hurricanes and anomalous heat in the Caribbean. *Geophys. Res. Lett.* **49**, e2022GL099740 (2022).
28. Wang, P. et al. Increasing compound hazards of tropical cyclones and heatwaves over southeastern coast of China under climate warming. *J. Clim.* **36**, 2243–2257 (2023).
29. Finney, D. L. et al. The effect of westerlies on East African rainfall and the associated role of tropical cyclones and the Madden–Julian Oscillation. *Q. J. R. Meteorol. Soc.* **146**, 3698 (2020).
30. Ding, Y. Summer monsoon rainfalls in China. *J. Meteor. Soc. Jpn.* **70**, 373–396 (1992).
31. Wang, B. & Ho, L. Rainy season of the Asian-Pacific summer monsoon. *J. Clim.* **15**, 386–398 (2002).
32. Ding, Y. *Advanced Synoptic Meteorology* (China Meteorological Press, 2005) (in Chinese).
33. Ding, Y. *Monsoons over China* (Kluwer Academic Publishers, 1992).
34. Zhang, J., Wu, L., Ren, F. & Cui, X. Changes in tropical cyclone rainfall in China. *J. Meteor. Soc. Jpn.* **91**, 585–595 (2013).
35. Li, C. et al. Relationship between summer rainfall anomalies and sub-seasonal oscillations in South China. *Clim. Dyn.* **44**, 423–439 (2015).
36. Zhang, Q. et al. Characteristics of drought in Southern China under climatic warming, the risk, and countermeasures for prevention and control. *Theor. Appl. Climatol.* **136**, 1157–1173 (2019).
37. Hu, Y. et al. Enhanced linkage of summer drought in southern China to the North Pacific oscillation since 2000. *J. Geophys. Res.* **128**, e2022JD037432 (2023).
38. Chang, C.-P. et al. Tropical cyclone and extreme rainfall trends in East Asian summer monsoon since mid-20th century. *Geophys. Res. Lett.* **39**, L18702 (2012).
39. Chen, J., Wu, R. & Wen, Z. Contribution of South China Sea tropical cyclones to an increase in southern China summer rainfall around 1993. *Adv. Atmos. Sci.* **29**, 585–598 (2012).
40. Liu, L. et al. Changes in tropical cyclone-induced extreme hourly precipitation over China during 1975–2018. *J. Clim.* **35**, 7339–7352 (2022).

41. Prat, O. P. & Nelson, B. R. On the link between tropical cyclones and daily rainfall extremes derived from global satellite observations. *J. Clim.* **29**, 6127–6135 (2016).
42. Chen, L., Li, Y. & Cheng, Z. An overview of research and forecasting on rainfall associated with landfalling tropical cyclones. *Adv. Atmos. Sci.* **27**, 967–976 (2010).
43. Liu, L. & Wang, Y. Trends in landfalling tropical cyclone–induced precipitation over China. *J. Clim.* **33**, 2223–2235 (2020).
44. Wang, X., Zhou, W., Li, C. Y. & Wang, D. X. Effects of the East Asian summer monsoon on tropical cyclone genesis over the South China Sea on an interdecadal time scale. *Adv. Atmos. Sci.* **29**, 249–262 (2012).
45. Yu, H. & Kwon, H. J. Effect of TC–trough interaction on the intensity change of two typhoons. *Weather Forecast.* **20**, 199–211 (2005).
46. Arakane, S. & Hsu, H.-H. A tropical cyclone removal technique based on potential vorticity inversion to better quantify tropical cyclone contribution to the background circulation. *Clim. Dyn.* **54**, 3201–3226 (2020).
47. Arakane, S. & Hsu, H.-H. Tropical cyclone footprints in long-term mean state and multiscale climate variability in the western North Pacific as seen in the JRA-55 reanalysis. *J. Clim.* **34**, 7443–7460 (2021).
48. Yamazaki, N. & Chen, T.-C. Analysis of the East Asian monsoon during early summer of 1979: Structure of the Baiu front and its relationship to large-scale fields. *J. Meteor. Soc. Jpn.* **71**, 339–355 (1993).
49. Kosaka, Y. & Nakamura, H. Structure and dynamics of the summertime Pacific–Japan teleconnection pattern. *Q. J. R. Meteor. Soc.* **132**, 2009–2030 (2006).
50. Kosaka, Y. & Nakamura, H. Mechanisms of meridional teleconnection observed between a summer monsoon system and a subtropical anticyclone. Part I: The Pacific–Japan pattern. *J. Clim.* **23**, 5085–5108 (2010).
51. Lu, R. & Lin, Z. Role of subtropical precipitation anomalies in maintaining the summertime meridional teleconnection over the western North Pacific and East Asia. *J. Clim.* **22**, 2058–2072 (2009).
52. Mei, W. & Xie, S. P. Intensification of landfalling typhoons over the northwest Pacific since the late 1970s. *Nat. Geosci.* **9**, 753–757 (2016).
53. Bhatia, K. T. et al. Recent increases in tropical cyclone intensification rates. *Nat. Commun.* **10**, 635 (2019).
54. Baker, A. J. Global decline in frequency. *Nat. Clim. Change* **12**, 615–617 (2022).
55. Chand, S. S. et al. Declining tropical cyclone frequency under global warming. *Nat. Clim. Change* **12**, 655–661 (2022).
56. Murakami, H. & Wang, B. Patterns and frequency of projected future tropical cyclone genesis are governed by dynamic effects. *Commun. Earth Environ.* **3**, 77 (2022).
57. Bender, M. A. et al. Modeled impact of anthropogenic warming of the frequency of intense Atlantic hurricanes. *Science* **327**, 454–458 (2010).
58. Knutson, T. R. et al. Simulated reduction in Atlantic hurricane frequency under twenty-first-century warming conditions. *Nat. Geosci.* **1**, 359–364 (2008).
59. Wu, J. & Gao, X. A gridded daily observation dataset over China region and comparison with the other datasets (in Chinese). *Chin. J. Geophys.* **56**, 1102–1111 (2013).
60. Kobayashi, S. et al. The JRA-55 reanalysis: general specifications and basic characteristics. *J. Meteor. Soc. Jpn.* **93**, 5–48 (2015).
61. Li, X., Wang, C. & Lan, J. Role of the South China Sea in southern China rainfall: meridional moisture flux transport. *Clim. Dyn.* **56**, 2551–2568 (2021).
62. Wu, R., Wen, Z., Yang, S. & Li, Y. An interdecadal change in southern China summer rainfall around 1992/93. *J. Clim.* **23**, 2389–2403 (2010).
63. Wilks, D. S. Hypothesis testing. In *Statistical Methods in the Atmospheric Sciences* (Academic Press, 2006).
64. Zwiers, F. W. & von Storch, H. Taking serial correlation into account in tests of the mean. *J. Clim.* **8**, 336–351 (1995).

ACKNOWLEDGEMENTS

We thank the three anonymous reviewers for their valuable comments, which helped to improve this paper. This work was supported by the National Natural Science Foundation of China (Grant Nos. 42275041, 41721004, and 42375028) and Guangdong Major Project of Basic and Applied Basic Research (Grant No. 2020B0301030004).

AUTHOR CONTRIBUTIONS

X.L. and R.L. designed the research. X.L. wrote all the software and code, conducted all calculations and produced all the figures. R.L., G.C., and R.C. provided constructive criticism, ideas and additional analysis as the work evolved. All authors interpreted the results and wrote the paper.

COMPETING INTERESTS

The authors declare no competing interests.

ADDITIONAL INFORMATION

Supplementary information The online version contains supplementary material available at https://doi.org/10.1038/s41612-023-00534-9.

Correspondence and requests for materials should be addressed to Xinyu Li.

Reprints and permission information is available at http://www.nature.com/reprints

Publisher's note Springer Nature remains neutral with regard to jurisdictional claims in published maps and institutional affiliations.